Strand-Specific Modulation of UV Photoproducts in 5S rDNA by TFIIIA Binding and Their Effect on TFIIIA Complex Formation†

Xiaoqi Liu, Antonio Conconi, and Michael J. Smerdon*

Department of Biochemistry and Biophysics, Washington State University, Pullman, Washington 99164-4660

Received July 10, 1997; Revised Manuscript Received August 28, 1997⊗

ABSTRACT: The relationship between UV-induced photoproduct formation and transcription factor binding was studied in a 214 bp fragment containing the entire *Xenopus borealis* 5S rRNA gene. DNA mobility shift and DNase I footprinting show a strong inhibition of TFIIIA binding to UV-damaged 5S rDNA. An average of ∼2 cyclobutane pyrimidine dimers (CPDs) per 214 bp fragment, and a lesser amount of pyrimidine-pyrimidone (6-4) dimers, reduced the fraction of TFIIIA bound by ∼70%. Furthermore, irradiation of the TFIIIA/5S rDNA complex displaces TFIIIA at doses of 0.8−2 CPDs/fragment, indicating the complex is unable to accommodate UV photoproducts. UV photofootprinting of the 50 bp TFIIIA binding region of 5S rDNA (or ICR) shows that TFIIIA binding modulates photoproduct formation primarily in the template strand. Formation of CPDs at six different sites is strongly inhibited, while another CPD site is strongly enhanced, by TFIIIA binding. Most of these sites are located in one of three boxes (A, IE, or C) designated as TFIIIA contact sites in the ICR, while one site is between these boxes. Formation of (6-4) dimers is also inhibited at several sites in the template strand by TFIIIA binding. However, formation of photoproducts in the nontemplate strand is much less affected by TFIIIA binding, where only one CPD site is inhibited in the complex. These data indicate that formation of UV photoproducts in 5S rDNA can be markedly affected by TFIIIA binding, and complex formation is inhibited by UV photoproducts.

The negative effects of ultraviolet (UV)[1] light on cells result, in part, from photoproducts formed in DNA. The major, stable UV-induced photoproduct in DNA is the *cis-syn* cyclobutane pyrimidine dimer (or CPD), which is a classic example of a lethal, mutagenic, and carcinogenic DNA lesion (*1*−*3*). Pyrimidine-pyrimidone (6-4) dimers [(6-4)PD] are the second most prevalent stable UV-induced photoproducts in DNA, and have been shown to form mutation hot-spots in specific genes of both bacterial and mammalian cells (*2*, *4*, *5*). As the functional state of DNA in cells involves numerous interactions with proteins, such as histones and transcription factors, it is important to understand the relationship between DNA damage and DNA−protein interactions. These interactions can be divided into (a) the *effects of DNA damage on DNA*−*protein interactions*, and (b) the *effects of DNA*−*protein interactions on DNA damage formation.*

Previous studies on nucleosome DNA demonstrated that CPD formation is strongly modulated by the folding of DNA into nucleosomes, forming a striking 10.3 base average periodicity in nucleosome cores with a strong preference to form away from the histone surface (*6*, *7*). This pattern disappears following nucleosome unfolding in very low salt (*8*), implying that DNA bending around the histone octamer is (at least partially) responsible for the periodic pattern. In support of this notion, it was shown that bending of a random-sequence DNA fragment, following binding of λ repressor to sequences at each end of the fragment, yields a similar ∼10-base periodic pattern of UV photoproducts (*9*). Furthermore, DNA binding of the bulky chemical carcinogen benzo[*a*]pyrenediol epoxide (BPDE) is suppressed by the presence of histones, where adduct levels are especially low within the central region of the nucleosome after short reaction times (*10*).

Other studies have focused on the effects of DNA damage on specific DNA−protein interactions. It was shown that the human ribosomal RNA transcription factor hUBF binds with high affinity to cisplatin−DNA adducts in random-sequence DNA (*11*). The same was observed for transcription factor Sp1 binding to BPDE adducts in nontarget DNA sequences (*12*). On the other hand, BPDE adducts *within* the DNA binding domains of the target sequences of Sp1 and transcription factor AP-1 inhibit the binding of these proteins (*13*, *14*). Similar results have recently been observed for UV-induced DNA damage where incorporation of CPDs into DNA regulatory elements strongly inhibits transcription factor binding (*15*). UV-induced DNA damage was also shown to interfere with nucleosome formation (*16*, *17*), and CPDs are found positioned away from the histone surface in nucleosomes reconstituted with UV-damaged DNA (*18*, *19*). Recently, we have shown that the stability of nucleosomes on damaged DNA can depend markedly on the type of DNA lesion formed, where BPDE adducts significantly *enhance* nucleosome formation onto the *Xenopus borealis* 5S ribosomal gene (5S rDNA) and UV photoproducts *inhibit* nucleosome formation onto this sequence (*20*).

† This study was supported by NIH Grant ES02614 from the National Institute of Environmental Health Sciences.

* Corresponding author [509-335-6853 (phone)/509-335-9688 (FAX)/smerdon@mail.wsu.edu (e-mail)].

⊗ Abstract published in *Advance ACS Abstracts,* October 15, 1997.

[1] Abbreviations: CPD, *cis-syn* cyclobutane pyrimidine dimer; (6-4)-PD, pyrimidine-pyrimidone (6-4) dimer; TFIIIA, transcription factor IIIA; UV, ultraviolet; BPDE, benzo[*a*]pyrenediol epoxide; ICR, internal control region; IE, intermediate element; DTT, dithiothreitol.

S0006-2960(97)01673-5 CCC: $14.00

We have used the *Xenopus borealis* 5S rRNA gene as a model system to study protein−DNA interactions on damaged DNA, and will be used for future studies on DNA repair of protein−DNA complexes *in vitro*. The binding of transcription factor IIIA (TFIIIA) to 5S rDNA is the first step in the synthesis of 5S rRNA (21). TFIIIA is comprised of both DNA and RNA binding domains containing 9 tandemly repeated zinc finger motifs and an additional C-terminal domain of 60 amino acid residues (*22*, *23*). TFIIIA binds to the internal control region (ICR) of 5S rDNA, which is about 50 bp long extending from +45 to +95 (where +1 denotes the transcription initiation site) (Figure 1). The ICR has three subdomains of protein binding: an A-box from +50 to +64, an intermediate element (IE) from +67 to +72, and a C-box from +80 to +97 (24). Methylation protection studies and measurements of TFIIIA affinities to a series of substitution mutations within the ICR led to the identification of essential nucleotides for TFIIIA binding. The results indicate that the C-box is the primary determinant of specific TFIIIA binding (25). It was also shown that the N-terminal fingers (fingers 1−3) of TFIIIA bind strongly at the C-box, the C-terminal fingers (fingers 7−9) bind strongly at the A-box, and the three middle fingers (fingers 4−6) interact with the IE sequence (*26*).

In the present paper, we have addressed both questions regarding protein−DNA binding and DNA damage (see above) using the 5S rDNA model system and UV radiation (at 254 nm). DNA mobility shifts and DNase I footprinting were used to test the effect of photoproducts in 5S rDNA on TFIIIA binding, and variations of UV photofootprinting were used to determine the effect of TFIIIA binding on UV photoproduct formation.

MATERIALS AND METHODS

Enzymes and Chemicals. The [γ-^{32}P]ATP (3000 Ci/mmol) used in this study was obtained from New England Nuclear, *Eco*RI and *Hin*dIII were purchased from International Biotechnologies, and T4 DNA polymerase was purchased from Boehringer Mannheim. T4 endonuclease V (T4 endo V) was the generous gift of Dr. R. S. Lloyd (University of Texas Medical Branch, Galveston, TX), and *E. coli* DNA photolyase was the generous gift of Dr. A. Sancar (University of North Carolina, Chapel Hill, NC).

Recombinant TFIIIA Expression and Purification. The *E. coli* strain BL21(DE3), containing the expression vector for TFIIIA (pTA102), was kindly provided by Dr. D. Setzer (Case Western Reserve University, Cleveland, OH). The recombinant TFIIIA expression and purification were performed as described by Del Rio and Setzer (27), with minor modifications. Briefly, the overexpressed recombinant TFIIIA was first purified on an ion-exchange column (BioRex 70) from BioRad, followed by application to a Pharmacia Superose 12 column, to separate full-length TFIIIA from a 37 kDa C-terminal truncated contaminant (*27*). The dissociation constant (K_d) for binding to the 5S rDNA fragment (see below) was measured to be 0.2 nM by gel mobility shift analysis (e.g., see Figure 3A).

5S rDNA Preparation. After linearization of plasmid pKS-5S (*20*) with either *Eco*RI (for template strand labeling) or *Hin*dIII (for nontemplate strand labeling), DNA was dephosphorylated with calf intestinal alkaline phosphatase (Boehringer Mannheim), and labeled with [γ-^{32}P]ATP using T4 polynucleotide kinase (United States Biochemical). A second restriction enzyme digestion (*Hin*dIII for template strand labeling and *Eco*RI for nontemplate strand labeling) produced a single end-labeled DNA fragment containing the 5S rRNA gene (see Figure 1). The resulting 214 bp fragment was recovered from a 2% agarose preparative gel using a gel extraction kit (QIAEX) from QIAGEN, and dissolved in 10 mM Tris-HCl, pH 8.0.

Irradiation with UV Light. A 5 μL drop of a ~2 μg/mL solution of single end-labeled 214 bp 5S rDNA fragments was irradiated under a bank of four low-pressure Hg lamps (Sylvania, Model G30T8), providing predominantly 254-nm light at a flux of about 15 W/m^2. UV flux was measured with a Spectroline DM-254N UV meter (Spectronics Corp., Westbury, NY).

DNA Mobility Shift Assay. After UV irradiation, DNA was incubated with TFIIIA according to Del Rio and Setzer (*27*). Briefly, samples were mixed in 20 mM Tris-HCl, pH 7.5, 7 mM $MgCl_2$, 10 μM $ZnCl_2$, 70 mM KCl, 1 mM dithiothreitol (DTT), 0.1% Nonidet P-40, 100 μg/mL BSA, 5% glycerol, 0.5 mM phenylmethanesulfonyl fluoride, and a 10-fold excess of poly(dI-dC). Incubations were at 25 °C for 30 min. Reaction mixtures were applied directly to a 8 cm × 7.3 cm nondenaturing 6% polyacrylamide gel [0.12% bis(acrylamide)] containing 25 mM Tris, 0.2 M glycine, and 5% glycerol, with 25 mM Tris base, 0.2 M glycine as the running buffer. Electrophoresis was run at room temperature for 1 h at 120 V after preelectrophoresis (using the same conditions) for 10 min. Gels were vacuum-dried and exposed to phosphorimager screens (Molecular Dynamics). Well-resolved band intensities were determined by the volume integration method of the ImageQuant program (Molecular Dynamics).

DNase I Footprinting. After formation of the TFIIIA/5S rDNA complex, DNase I (0.4 unit) was added to the sample and incubated at room temperature for 90 s. The reaction was stopped by addition of an equal volume of 50 mM Tris-HCl, pH 8.0, 150 mM NaCl, 5 mM EDTA, 0.5% SDS, and 50 μg/mL mussel glycogen. Following phenol extraction and ethanol precipitation, DNA samples were run on 8% polyacrylamide/8 M urea sequencing gels (*27*). Gels were then dried and exposed to phosphorimager screens, as described above.

CPD Mapping. UV-irradiated 5S rDNA was dissolved in T4 endo V buffer [20 mM Tris-HCl (pH 7.4), 10 mM EDTA (pH 8.0), 100 mM NaCl, and 100 μg/mL BSA]. One microliter of a 100-fold dilution of T4 endo V stock (400 ng/μL) was added and incubated at 37 °C for 1 h. The reaction was stopped by the addition of gel loading buffer, followed by incubation in boiling water for 10 min. Reaction mixtures were loaded directly onto the gel (see below).

Photoreversal of CPDs. UV-damaged 5S rDNA was dissolved in 9 μL of photolyase reaction buffer (20 mM phosphate, pH 7.5, 2 mM EDTA, 0.1 mM DTT, and 125 mM NaCl), to which 1 μL of purified *E. coli* DNA photolyase stock (20 μg/mL) was added. After a 5-min preincubation in the dark, samples were placed on ice and exposed to photoreactivating light from a 450 W medium-pressure Hg lamp (Ace Glass Inc., Vineland, NJ) filtered with a 389 nm cutoff filter (SLM Instruments, Urbana Champaign, IL) for 1 h.

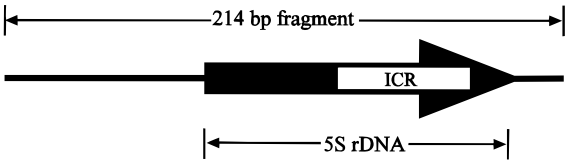

FIGURE 1: Schematic of the *Eco*RI−*Hin*dIII 5S rDNA fragment used in the study. The solid arrow designates the location of the 120 bp 5S rDNA, while the open box designates the 50 bp internal control region (i.e., the TFIIIA binding site).

Digestion with T4 DNA Polymerase. Digestion of 5S rDNA samples with T4 DNA polymerase was performed according to Gale and Smerdon (*7*). Briefly, after heat denaturation in boiling water for 10 min, DNA samples were dissolved in T4 DNA polymerase digestion buffer [50 mM Tris-HCl, pH 8.8, 15 mM $(NH_4)_2SO_4$, 7 mM $MgCl_2$, 0.1 mM EDTA, 10 mM 2-mercaptoethanol, and 0.2 mg/mL BSA] and incubated with 1 unit of T4 DNA polymerase (5000 units/mg of DNA activity) for 1 h at 37 °C. The reaction was stopped by heating at 65 °C for 10 min.

After digestion with either T4 DNA polymerase-exonuclease or T4 endo V, gel loading buffer was added to the reaction mixtures, and the samples were loaded onto 8% polyacrylamide/8 M urea sequencing gels (*6*). The same amount of ^{32}P DPMs were loaded into the wells, and the gels were run at 50 °C for 2 h at 1600 V.

RESULTS

CPD Yield in the 5S rDNA Fragment and TFIIIA/5S rDNA Complex. The average CPD yield in the 214 bp *Eco*RI−*Hin*dIII 5S rDNA fragment shown in Figure 1 was determined for different UV doses from the fraction of 5S rDNA fragments resistant to T4 endo V (e.g., see *28*), which cuts DNA strands specifically at CPDs (*29*). Irradiation of naked DNA fragments, with only one strand end-labeled, indicates that the average CPD yield is higher in the template strand than in the nontemplate strand at the higher UV doses used [Figure 2B (compare lanes 2 and 4 with lanes 10 and 12)]. Indeed, quantitation of the uncleaved 214 bp band intensity indicates almost 50% more CPDs form in the template strand at UV doses >1 kJ/m^2 [Figure 2C,D (hatched bars)]. This difference cannot be entirely accounted for by the higher TC content in the template strand (53%), compared to the nontemplate strand (47%), and must reflect additional features of this fragment when free in solution.

Binding of purified TFIIIA to 5S rDNA yields a noticeable retardation in 5S rDNA migration in nondenaturing acrylamide gels, and this can be used to determine the ratio of bound and free 5S rDNA (Figure 2A). In agreement with past reports (*27*), we find a mole ratio of ∼2:1 (TFIIIA:5S rDNA) gives near-complete complex formation (Figure 2A). These conditions were used to examine the average CPD formation in the TFIIIA/5S rDNA complex following different UV doses (Figure 2B−D). As shown in Figure 2B (lanes 5−8 and 13−16), TFIIIA binding reduces the CPD yield in the template strand of 5S rDNA, while there is less of an effect on the nontemplate strand (compare +TFIIIA lanes with −TFIIIA lanes for each strand). Quantitation of the 214 bp band intensity shows a marked reduction of CPDs in the template strand of the complex, compared with naked DNA, at all but the lowest UV doses tested (Figure 2C; compare solid and hatched bars). Conversly, only a small

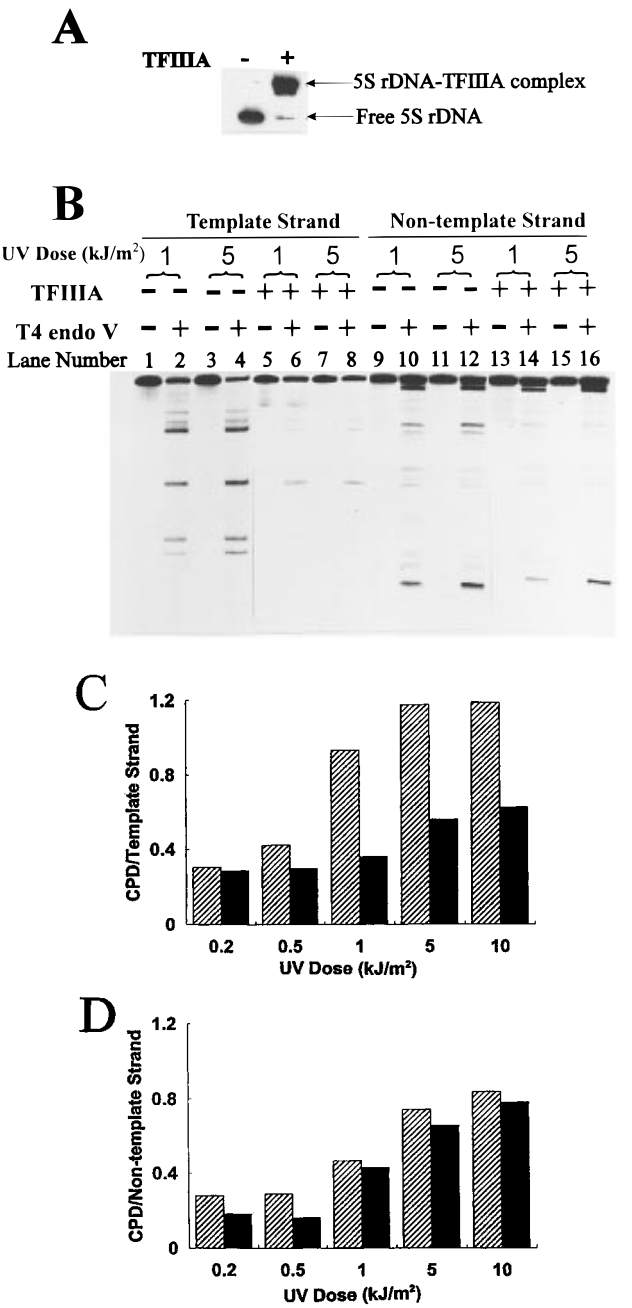

FIGURE 2: Effect of TFIIIA binding on average CPD yield. (A) Band shift of 214 bp 5S rDNA fragment with (+) and without (−) TFIIIA at the [protein]/[DNA] ratio used in panel B. Samples were mixed and run on a nondenaturing polyacrylamide gel as described under Materials and Methods. (B) CPD yield in end-labeled 5S rDNA (−TFIIIA) or 5S rDNA−TFIIIA complex (+TFIIIA) following irradiation at two different UV doses. 5S rDNA was end-labeled on the template or nontemplate strand, incubated with (+) or without (−) TFIIIA ([protein]/[DNA] = 2), irradiated with UV light, purified and incubated with (+) or without (−) T4 endo V, and run on sequencing gels. Shown is the phosphorimage of T4 endo V cut fragments for the template (lanes 1−8) and nontemplate (lanes 9−16) strands. (C, D) Results of quantitation of (214 base) band intensities on phosphorimages for the template and nontemplate strands (see Materials and Methods). Values are the average of two separate experiments in each case. Hatched bars indicate overall CPD yields in free DNA, and solid bars indicate overall CPD yields in the TFIIIA−5S rDNA complex.

reduction is observed for the nontemplate strand following TFIIIA binding (Figure 2D). As shown below, this reflects inhibition of CPD formation at specific sites in the TFIIIA binding region (or ICR).

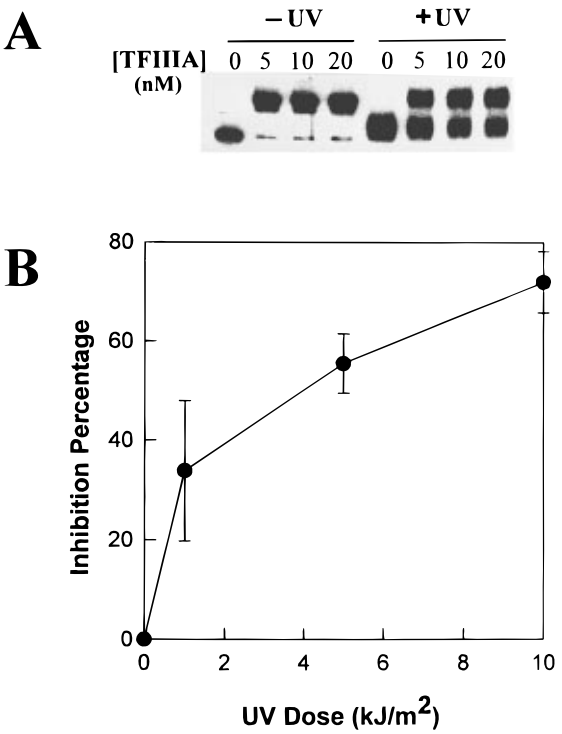

FIGURE 3: Effect of UV damage on TFIIIA−5S rDNA band shift. (A) Representative autoradiogram of end-labeled 214 bp 5S rDNA fragment at a fixed concentration of 1 nM, incubated with increasing amounts of TFIIIA (0, 5, 10, 20 nM) at 25 °C for 30 min. The complexes were directly loaded onto a nondenaturing polyacrylamide gel, and run for 1.5 h. The left four lanes are for unirradiated 5S rDNA (−UV), while the right four lanes are for 5S rDNA irradiated with 10 kJ/m^2 UV light prior to incubation with TFIIIA (+UV). (B) Results for quantitation of autoradiograms from four separate experiments (mean ± 1 SD). Inhibition percentage was calculated from the equation: [1 − (bound/free)$_{+UV}$/(bound/free)$_{-UV}$] × 100, where (bound/free) represents the ratio between the intensity of the slow migrating band and the intensity of the fast migrating band.

TFIIIA Binding to UV-Damaged 5S rDNA. The DNA mobility shift analyses showed that UV damage strongly inhibits TFIIIA binding (Figure 3A). Complex formation on 5S rDNA, irradiated with 10 kJ/m^2 UV light, is inhibited by over 70% compared to unirradiated fragments (Figure 3B). At this high UV dose, there is an average of about 2 CPDs formed in the 214 bp fragment (e.g., see Figure 2C,D)- and, therefore, significantly less in the 50 bp TFIIIA binding region (ICR). In addition, DNase I footprinting of the complex also showed a strong inhibition of TFIIIA binding following the higher UV doses (5−10 kJ/m^2), where average levels approached 1 CPD/fragment strand (Figure 4). Moreover, the DNase I footprinting experiments show that UV inhibition of TFIIIA/5S rDNA complex formation involves the entire 50 bp ICR region (Figure 4, arrow), and TFIIIA does not occupy one (or two) of the interior DNA boxes while being partly displaced by UV photoproducts (Figure 4). Together, these data clearly show that photoproduct formation in the 5S rRNA gene inhibits TFIIIA binding.

We also asked if UV photodamage in 5S rDNA can displace a *preexisting* complex. As shown in Figure 5, UV irradiation at doses >1 kJ/m^2 displaces TFIIIA from the 5S rDNA complex similar to the UV doses that inhibit complex formation (Figure 3). Thus, it appears that the TFIIIA/5S rDNA complex cannot tolerate UV photolesions (in at least some sites) in the DNA, and the energy penalty is too great to maintain a complex containing a UV photoproduct. This could be explained by an increased off-rate during the equilibrium of TFIIIA and UV-damaged DNA or a decreased on-rate, where rebinding of TFIIIA is only to undamaged DNA molecules.

UV Photoproduct Formation at Specific Sites in 5S rDNA following TFIIIA Binding. The effect of TFIIIA binding on UV photoproduct formation at the nucleotide level in 5S rDNA was examined using an exonuclease blockage assay referred to as UV photofootprinting (*6*, *30*, *31*). T4 polymerase (or T4 pol-exo) possesses a 3′→5′ exonuclease activity in the absence of deoxyribonucleotide triphosphates and hydrolyzes both single- and double-strand DNA (*32*). This exonuclease is quantitatively blocked by both CPDs and (6-4)PDs (*30*). Figure 6A shows an example of UV photofootprinting of the 5S rDNA template strand irradiated at four different UV doses. Even after the low UV dose of 100 J/m^2 (lane 1), where only about 10% of the DNA fragments contain CPDs, the enzyme blockage sites (gel bands) are easily detected. When these gel lanes are compared with the sequencing lanes (lanes 5−8), a 1−2 base shift (decrease) in gel migration is observed from that of adjacent pyrimidine sites in the sequencing lanes. This indicates that T4 pol-exo stops 1−2 bases 3′ of the photoproducts (Figure 6A), in agreement with Gale and Smerdon (*7*).

To differentiate between CPD- and (6-4)PD-forming sites in the ICR, we used T4 endo V to specifically cut at CPDs and a combination of UV photolyase and T4 pol-exo to detect (6-4)PDs (e.g., see *31*). Representative results are shown in Figure 6B (lanes 2−4, 6−8, 10−12, and 14−16) for varied amounts of complex formation. These results were compared with the gel patterns obtained for irradiated 5S rDNA (Figure 6B; lanes 1, 5, 9, and 13). As can be seen, there are several CPD sites in the template strand that are reduced in yield following complex formation (Figure 6B, see stars on left). In addition, there is one site that is enhanced in quantum yield in the complex (Figure 6B, open square). Quantitation of these sites, after correction for loading differences (see Materials and Methods), shows that six different sites have over 40% less CPDs in the complex than in naked 5S rDNA (Figure 8, solid bars). In addition, two sites have at least 20% *more* CPDs than in naked 5S rDNA (Figure 8, open bars). Overall, there are at least 11 (out of 13 total) CPD sites in the template strand of the 50 bp ICR region that are modulated by TFIIIA binding. Most of these sites are located in one of the three boxes (A, IE, or C), while only one site (at T74C75) is between the C-box and intermediate element (see Figure 8).

Similar experiments were performed with the nontemplate strand labeled at the 5′ end (Figure 7). In this case, there is only one obvious site (out of five total) in the nontemplate strand where TFIIIA binding affects the CPD yield (Figure 7B, see star). As shown in Figure 8 (bottom strand), this site is at the 5′ edge of the C-box and contains over 50% less CPDs in the complex than in naked 5S rDNA. The remainder of the photoproduct sites in the nontemplate strand had more than 90% of the yield found in naked 5S rDNA (Figure 8). Thus, only one photoproduct site (a CPD at the edge of the C-box) is significantly reduced in the nontemplate strand of the ICR following TFIIIA binding.

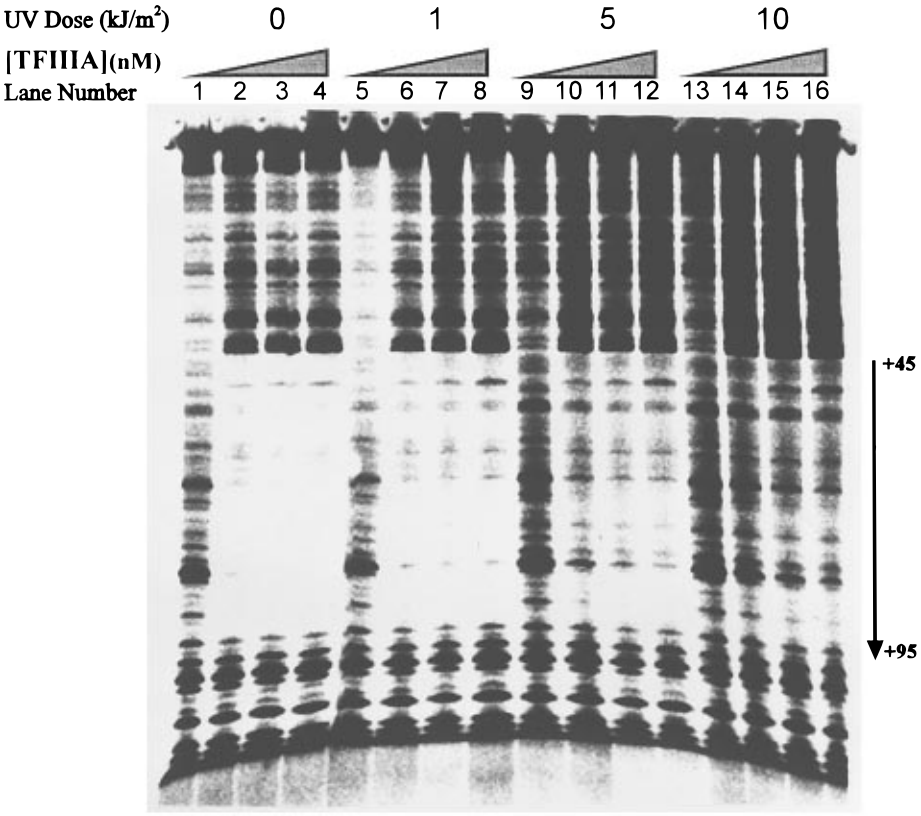

FIGURE 4: Effect of UV damage on TFIIIA−5S rDNA footprint. After irradiation with increasing UV doses [0 kJ/m^2 (lanes 1−4), 1 kJ/m^2 (lanes 5−8), 5 kJ/m^2 (lanes 9−12) to 10 kJ/m^2 (lanes 13−16)], the DNA samples (10 nM) were incubated with different amounts of TFIIIA (0, 10, 20, 40 nM) to form varying ratios of complexes to free 5S rDNA. Samples were incubated with DNase I (0.4 unit) at room temperature for 90 s, and the reactions were stopped with equal volumes of 5 mM EDTA. The TFIIIA binding site (or ICR) is indicated by the arrow on the right.

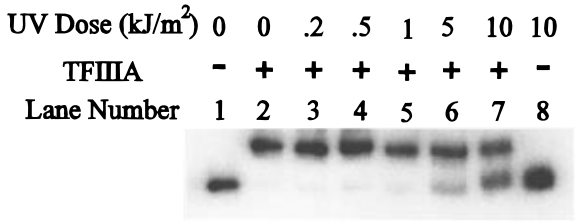

FIGURE 5: UV irradiation disrupts TFIIIA−5S rDNA complexes. Complexes were formed as described in Figures 2−4, irradiated with 0, 0.2, 0.5, 1, 5, or 10 kJ/m^2 UV light, and run on a nondenaturing polyacrylamide gel.

DISCUSSION

It has been known for over 2 decades that UV radiation inhibits RNA synthesis (*33*). Mayne and Lehmann (*34*) showed that this synthesis rapidly returns following post-UV incubation, and Mellon et al. (*35*) showed this was due to preferential repair of the transcribed strand of RNA pol II genes. Furthermore, Selby and Sancar demonstrated that a single CPD in the transcribed strand inhibits transcription by forming a block to elongating RNA pol II (*36*), and preferential repair of this block in *E. coli* requires a transcription−repair coupling factor (*37*). Another possible mechanism for UV inhibition of gene expression is inhibition of transcription factor binding to target sequences by DNA photoproducts (*38*). In the present study, we tested the effect of UV damage on transcription factor TFIIIA binding to 5S rDNA. We show that TFIIIA binding is markedly inhibited following UV doses that induce 0.8−2 CPDs/214 bp fragment (Figure 3), where the actual level of photoproducts in the 50 bp TFIIIA binding region (ICR) is even lower.

The effect of chemical DNA adducts on transcription factor binding has been analyzed previously for other systems, and the effects depend on both the type of DNA damage and the target sequences studied. It was demonstrated that the high-mobility group protein HMG1 and human upstream binding factor (hUBF) bind mixed-sequence DNA substrates containing a cisplatin adduct with very high affinity (*11*, *39*). On the other hand, alkylation of DNA was shown to inhibit binding of several transcription factors, including NFκB, Sp1, OTF-1, and AP2 (*40*−*43*). Furthermore, during preparation of this paper, the effect of UV damage on transcription factor binding was reported for the first time (*15*). It was shown that incorporation of CPDs into specific sites of oligonucleotides strongly inhibits binding of the sequence-specific transcription factors E2F, NF-Y, AP-1, NFκB, and p53 (*15*). Here, we show that UV damage can also dramatically inhibit binding of TFIIIA to 5S rDNA, a transcription factor required for RNA polymerase III expression. Therefore, it seems that the binding of many different transcription factors can be inhibited by UV radiation, suggesting that UV-induced photoproducts could alter regulation of a large number of genes. This inhibition may be due to a conformational change in the recognition sequence upon photoproduct formation. Indeed, NMR and gel retardation experiments show that CPDs cause a 7°−9° bend in the long axis of double-stranded DNA fragments (*44*, *45*), while an ∼44° bend is observed at a (6-4)PD site in a double-stranded dodecamer (*45*). Clearly,

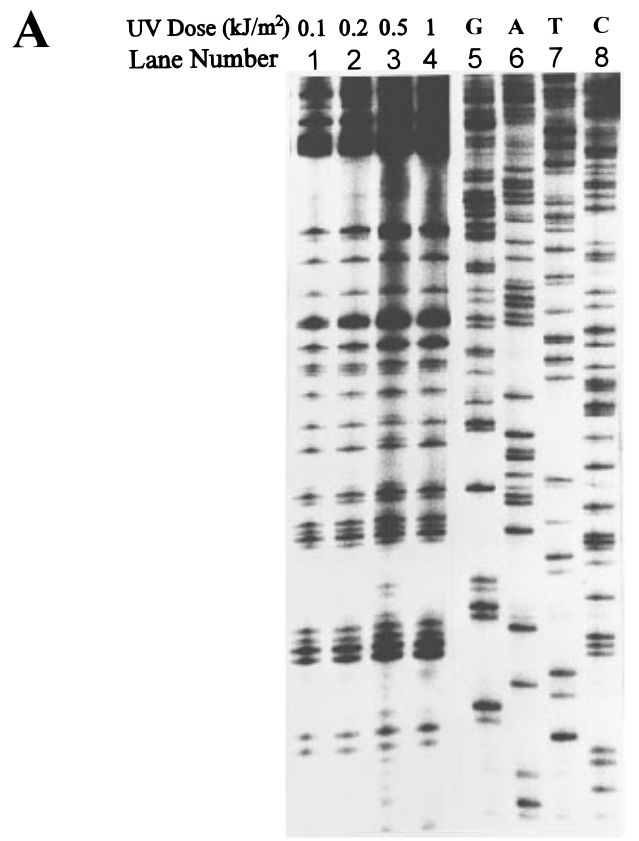

FIGURE 6: Modulation of UV photoproducts in the template strand of 5S rDNA by TFIIIA binding. (A) UV photoproduct distribution in the template strand following different UV doses. Naked 5S rDNA, end-labeled on the template strand, was irradiated with different UV doses and subjected to T4 poly-exo digestion (lanes 1−4). Dideoxynucleotide sequenase reactions are shown in lanes 5−8. (B) Effect of TFIIIA binding on UV photofootprint of the template strand. The 5S rDNA fragments (10 nM) were incubated with increasing amounts of TFIIIA (0, 20, 40, 60 nM) to form different amounts of complexes (lanes 1, 5, 9, and 13 are for no complexes), and irradiated with 1 kJ/m^2 UV light. Purified DNA samples were digested with T4 pol-exo (lanes 1−4), T4 endo V (lanes 5−8), or T4 pol-exo after incubation with UV photolyase to remove CPDs (lanes 9−12). An aliquot of the complexes was also digested with DNase I (lanes 13−16). Lane G is the sequenase reaction lane for dideoxyguanidine. Strong inhibition sites are indicated by stars (at left), and the open square denotes a site of enhanced CPD formation in the complex. The arrow to the right denotes the TFIIIA binding region.

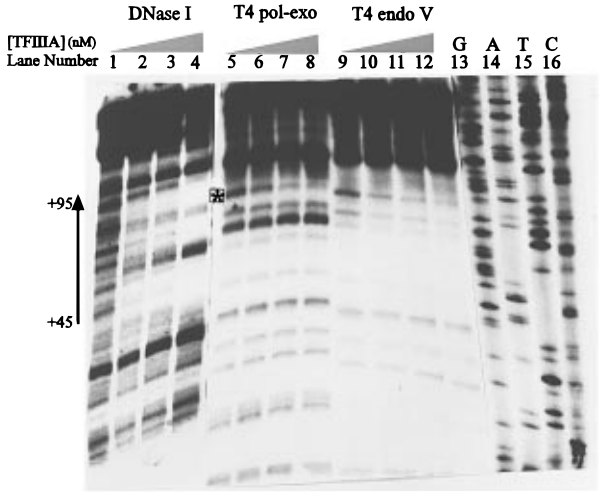

FIGURE 7: Modulation of UV photoproducts in the nontemplate strand of 5S rDNA by TFIIIA binding. 5S rDNA fragments, end-labeled on the nontemplate strand, were incubated with increasing amounts of TFIIIA and irradiated with 1 kJ/m^2 UV light as described for Figure 6B. Purified DNA samples were digested with T4 pol-exo (lanes 5−8) or T4 endo V (lanes 9−12). A DNase I digest of the complex is also shown (lanes 1−4), and the sequenase reactions are shown in lanes 13−16. The star (left of lane 5) denotes a strong CPD inhibition site, and the TFIIIA binding region is indicated by the arrow at the left.

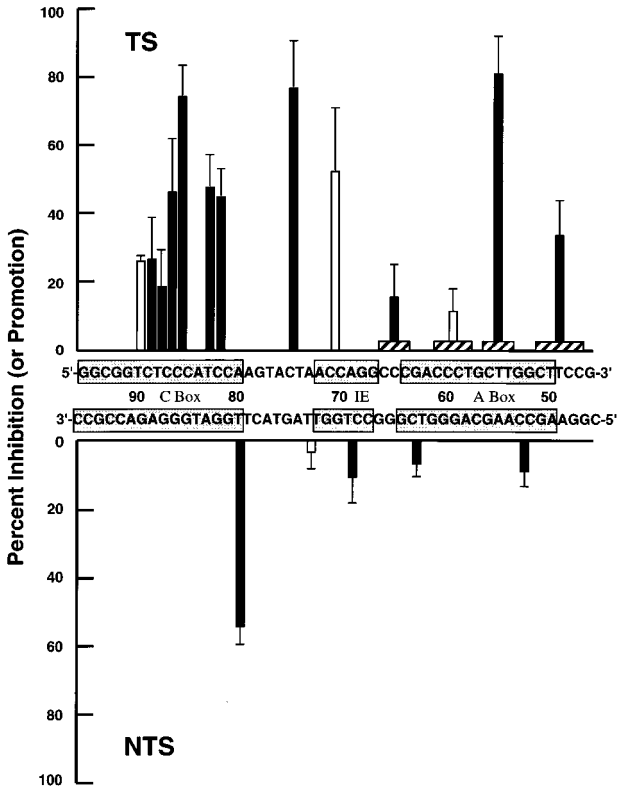

FIGURE 8: Summary of the effect of TFIIIA binding on CPD formation in the ICR region of 5S rDNA. Data represent the mean ± 1 SD (8 experiments for template strand and 4 experiments for nontemplate strand), and the bars above the sequence represent data from the template strand and the bars below the sequence represent data from the nontemplate strand. The locations of the C-box, IE, and A-box are denoted by stippled boxes on each strand. Inhibition and promotion of CPD formation by TFIIIA binding are represented by solid and open bars, respectively. Average values for pyrimidine tracts are denoted by horizontal (hatched) boxes over the top strand.

such bending at UV photoproducts may not be compatible with the conformation of the TFIIIA−5S rDNA complex.

DNA−protein interactions can also modulate UV photoproduct formation, as found within nucleosome cores (*6*−*8*, *46*). Modulation of UV photoproducts was also observed in the DNA binding sequences for c-*jun*, c-*fos*, and PCNA (*47*). Thus, modulation of UV photoproducts may be a general phenomenon of protein binding, especially in transcription factor binding sites where pyrimidine-tracts frequently occur (*48*). Previously, Wang and Becker (*49*) observed inhibition of UV photoproduct formation in the template strand of sea urchin 5S rDNA following TFIIIA binding (no comparison was made with the nontemplate strand). The chemical cleavage method used by these authors, however, was not specific for pyrimidine dimers and produced significant cleavage of unirradiated DNA (*50*). Here, we show that following TFIIIA binding this modulation is strand-specific, in agreement with current models for the TFIIIA−5S rDNA complex (*51*−*53*), where strong contacts with TFIIIA are observed only with the template strand. Furthermore, quantitative analysis of the photoproduct distributions indicates that within the template strand, the modulation pattern is not uniform (Figure 8). There is strong inhibition (>40% inhibition) at four CPD sites in the C-box region, while only one CPD site is strongly inhibited in the A-box region (Figure 8). Interestingly, the C-box region of the ICR, which forms contacts with the N-terminal fingers of TFIIIA (fingers 1−3), has been shown to be the most important region for accurate TFIIIA binding (*25*).

We also observed modulation of photoproducts at other sites in the ICR (i.e., outside the C-box region). For example, CPD formation is strongly inhibited at one site in the template strand of the A-box region (at T54T55) following TFIIIA binding. These two bases do not form direct contacts with any zinc fingers in TFIIIA; however, finger 8 makes contacts with the bases C47C48T49 and T58C59 on each side of this site (*53*). The binding to finger 8 may restrict the flexibility of T54 and T55 between the two bases required for CPD formation. In addition, in regions where multiple dimer-forming sites exist next to each other and these sites were not resolved (Figure 8; e.g., near T49T50), "moderate" inhibition by TFIIIA binding may actually reflect a direct interaction with TFIIIA (and therefore a strong modulation) at only some of the sites, while other sites in this region are less affected.

In the IE region of the ICR, CPD formation is enhanced at one site in the template strand (C70C71) upon TFIIIA binding (Figure 8). The binding of the three middle zinc fingers (fingers 4−6) of TFIIIA to this region is different than the binding of the other fingers to the ICR (*52*). In fact, both the N- and C-terminal fingers (fingers 1−3 and 7−9, respectively) wrap along the major groove of DNA, while the three middle fingers (fingers 4−6) form a unit that runs nearly parallel to the helix axis in the center of the complex. It was proposed that this unit is in position to interact with bases on one side of the DNA helix in the major groove (centered at A69 on the template strand and A74/G75 on the nontemplate strand). Thus, the enhanced CPD formation at site C70C71 following TFIIIA binding suggests that the interaction of TFIIIA with 5S rDNA causes bending that facilitates CPD formation. Indeed, TFIIIA has been shown to induce a substantial distortion in the structure of 5S rDNA upon binding (*54*).

Two CPD sites that are strongly modulated (T74C75 in the template strand and T79T80 in the nontemplate strand) are not in the three binding elements (Figure 8). Bases T74C75 in the template strand have relatively weak contacts with TFIIIA and T79T80 in the nontemplate strand are not in direct contact with any zinc fingers of the protein (*52*, *53*). These two sites are on the edge of the IE and C-box regions, respectively, and the TFIIIA contacts within these nearby elements may restrict the flexibility of bases at these two sites. Clearly, a complete explanation of these results must await a high-resolution crystal structure of the TFIIIA−5S rDNA complex.

Finally, it is possible that only some photoproduct sites in the ICR are responsible for displacing TFIIIA (see Figure 5). Indeed, some sites are inhibited much more than others in the complex (Figure 6B). Therefore, it may be the sites that form most efficiently in the complex that cause the displacement of TFIIIA, and are most effective at altering 5S RNA transcription in cells. To date, very little is known about the inhibition of pol III gene expression by UV photoproducts, and it was only recently reported that, unlike RNA polymerase II, RNA polymerase III transcription does not stimulate excision repair (*55*).

ACKNOWLEDGMENT

We thank Dr. D. Setzer for providing *E. coli* B strain BL21(DE3) with the cloned TFIIIA gene, Dr. A. Sancar for providing *E. coli* DNA photolyase, and Dr. R. S. Lloyd for supplying purified T4 endo V. We also thank C. Suquet for technical assistance and members of the Smerdon laboratory for helpful discussions.

REFERENCES

1. Harm, W. (1980) *Biological Effects of Ultraviolet Radiation*, Cambridge University Press, London.
2. Brash, D. E. (1988) *Photochem. Photobiol. 48*, 59−66.
3. Cadet, J., Anselmino, C., Douki, T., and Voituriez, L. (1992) *J. Photochem. Photobiol. B: Biol. 15*, 277−298.
4. Mitchell, D. L., and Nairn, R. S. (1989) *Photochem. Photobiol. 49*, 805−819.
5. Mullenders, L. H. F., Hazekamp-van Dokkum, A. M., Kalle, W. H. J., Vrieling, H., Zdzienicka, M. Z., and van Zeeland, A. A. (1993) *Mutat. Res. 299*, 271−276.
6. Gale, J. M., Nissen, K. A., and Smerdon, M. J. (1987) *Proc. Natl. Acad. Sci. U.S.A. 84*, 6644−6648.
7. Gale, J. M., and Smerdon, M. J. (1988) *J. Mol. Biol. 204*, 949−958.
8. Brown, D. W., Libertini, L. J., Suquet, C., Small, E. W., and Smerdon, M. J. (1993) *Biochemistry 32*, 10527−10531.
9. Pehrson, J. R., and Cohen, L. H. (1992) *Nucleic Acids Res. 20*, 1321−1324.
10. Thrall, B. D., Mann, D. B., Smerdon, M. J., and Springer, D. L. (1994) *Biochemistry 33*, 2210−2216.
11. Treiber, D. K., Zhai, X., Jantzen, H. M., and Essigmann, J. M. (1994) *Proc. Natl. Acad. Sci. U.S.A. 91*, 5672−5676.
12. MacLeod, M. C., Powell, K. L., and Tran, N. (1995) *Carcinogenesis 16*, 975−983.
13. MacLeod, M. C., Powell, K. L., Kuzmin, V. A., Kolbanovskiy, A., and Geacintov, N. E. (1996) *Mol. Carcinog. 16*, 44−52.
14. Persson, A. E., Pontén, I., Cotgreave, I., and Jernström, B. (1996) *Carcinogenesis 17*, 1963−1969.
15. Tommasi, S., Swiderski, P. M., Tu, Y., Kaplan, B. E., and Pfeifer, G. P. (1996) *Biochemistry 35*, 15693−15703.
16. Matsumoto, H., Takakusu, A., and Ohnishi, T. (1994) *Photochem. Photobiol. 60*, 134−138.
17. Matsumoto, H., Takakusu, A., Mori, T., Ihara, M., Todo, T., and Ohnishi, T. (1995) *Photochem. Photobiol. 61*, 459−462.
18. Suquet, C., and Smerdon, M. J. (1993) *J. Biol. Chem. 268*, 23755−23757.

19. Schieferstein, U., and Thoma, F. (1996) *Biochemistry 35*, 7705−7714.
20. Mann, D. B., Springer, D. L., and Smerdon, M. J. (1997) *Proc. Natl. Acad. Sci. U.S.A. 94*, 2215−2220.
21. Wolffe, A. P., and Brown, D. D. (1988) *Science 241*, 1626−1632.
22. Smith, D. R., Jackson, I. J., and Brown, D. D. (1984) *Cell 37*, 645−652.
23. Miller, J., McLachlan, A. D., and Klug, A. (1985) *EMBO J. 4*, 1609−1614.
24. Clemens, K. R., Zhang, P., Liao, X., McBryant, S. J., Wright, P. E., and Gottesfeld, J. M. (1994) *J. Mol. Biol. 244*, 23−35.
25. You, Q., Veldhoen, N., Baudin, F., and Romaniuk, P. J. (1991) *Biochemistry 30*, 2495−2500.
26. Vrana, K. E., Churchill, M. E. A., Tullius, T. D., and Brown, D. D. (1988) *Mol. Cell. Biol. 8*, 1684−1696.
27. Del Rio, S., and Setzer, D. R. (1991) *Nucleic Acids Res. 19*, 6197−6203.
28. Bohr, V. A., and Okumoto, D. S. (1988) *DNA Repair: A Laboratory Manual of Research Procedures* (Friedberg, E. C., and Hanawalt, P. C., Eds.) pp 347−366, Marcel Dekker, Inc., New York.
29. Friedberg, E. C., Walker, G. C., and Siede, W. (1995) *DNA Repair and Mutagenesis*, American Society for Microbiology Press, Washington, D.C.
30. Doetsch, P. W., Chan, G. L., and Haseltine, W. A. (1985) *Nucleic Acids Res. 13*, 3285−3304.
31. Gale, J. M., and Smerdon, M. J. (1990) *Photochem. Photobiol. 51*, 411−417.
32. Huang, W. M., and Lehman, I. R. (1972) *J. Biol. Chem. 247*, 3139−3146.
33. Sauerbier, W. (1976) *Adv. Radiat. Biol. 6*, 49−106.
34. Mayne, L. V., and Lehmann, A. R. (1982) *Cancer Res. 42*, 1473−1478.
35. Mellon, I., Spivak, G., and Hanawalt, P. C. (1987) *Cell 51*, 241−249.
36. Selby, C. P., and Sancar, A. (1990) *J. Biol. Chem. 265*, 21330−21336.
37. Selby, C. P., and Sancar, A. (1993) *Science 260*, 53−58.
38. Pfeifer, G. P. (1997) *Photochem. Photobiol. 65*, 270−283.
39. Pil, P. M., and Lippard, S. J. (1992) *Science 256*, 234−237.
40. Bonfanti, M., Broggini, M., Prontera, C., and D'Incalci, M. (1991) *Nucleic Acids Res. 19*, 5739−5742.
41. Fabbri, S., Prontera, C., Broggini, M., and D'Incalci, M. (1993) *Carcinogenesis 14*, 1963−1967.
42. Sun, D., and Hurley, L. H. (1994) *Gene 149*, 165−172.
43. Gray, P. J. (1995) *Nucleic Acids Res. 23*, 4378−4382.
44. Wang, C.-I., and Taylor, J.-S. (1991) *Proc. Natl. Acad. Sci. U.S.A. 88*, 9072−9076.
45. Kim, J.-K., Patel, D., and Choi, B.-S. (1995) *Photochem. Photobiol. 62*, 44−50.
46. Pehrson, J. R. (1989) *Proc. Natl. Acad. Sci. U.S.A. 86*, 9149−9153.
47. Tornaletti, S., and Pfeifer, G. P. (1995) *J. Mol. Biol. 249*, 714−728.
48. Faisst, S., and Meyer, S. (1992) *Nucleic Acids Res. 20*, 3−26.
49. Wang, Z., and Becker, M. M. (1988) *Proc. Natl. Acad. Sci. U.S.A. 85*, 654−658.
50. Becker, M. M., and Wang, Z. (1989) *J. Mol. Biol. 210*, 429−438.
51. Sakonju, S., and Brown, D. D. (1982) *Cell 31*, 395−405.
52. Hayes, J. J., and Tullius, T. D. (1992) *J. Mol. Biol. 227*, 407−417.
53. Del Rio, S., Menezes, S. R., and Setzer, D. R. (1993) *J. Mol. Biol. 233*, 567−579.
54. Schroth, G. P., Cook, G. R., Bradbury, E. M., and Gottesfeld, J. M. (1989) *Nature 340*, 487−488.
55. Dammann, R., and Pfeifer, G. P. (1997) *Mol. Cell. Biol. 17*, 219−229.

BI9716736